Determination of transport stoichiometry for two cation-coupled *myo*-inositol cotransporters: SMIT2 and HMIT

Francis Bourgeois, Michael J. Coady and Jean-Yves Lapointe

Groupe d'étude des protéines membranaires (GÉPROM) and Département de Physique, Université de Montréal, Canada

Three different mammalian *myo*-inositol cotransporters are currently known; two are Na^+-coupled (SMIT1 and SMIT2) and one is proton-coupled (HMIT). Although their transport stoichiometries have not been directly determined, significant cooperativities in the Na^+ activation of SMIT1 and SMIT2 suggest that more than one Na^+ ion drives the transport of each *myo*-inositol. The two techniques used here to determine transport stoichiometry take advantage of the electrogenicity of both SMIT2 and HMIT expressed in *Xenopus* oocytes. The first method compares the measurement of charge transferred into voltage-clamped oocytes with the simultaneous uptake of radiolabelled substrate. The second approach uses high accuracy volume measurements to determine the transport-dependent osmolyte uptake and compares it to the amount of charge transported. This method was calibrated using a potassium channel (ROMK2) and was validated with the Na^+/glucose cotransporter SGLT1, which has a known stoichiometry of 2 : 1. Volume measurements indicated a stoichiometric ratio of 1.78 ± 0.27 ion per α-methyl-glucose (αMG) for SGLT1 whereas the radiotracer uptake method indicated 2.14 ± 0.05. The two methods yielded a SMIT2 stoichiometry measurement of 1.75 ± 0.30 and 1.82 ± 0.10, both in agreement with a 2 Na^+:1 *myo*-inositol stoichiometry. For HMIT, the flux ratio was 1.02 ± 0.04 charge per *myo*-inositol, but the volumetric method suggested 0.67 ± 0.05 charge per *myo*-inositol molecule. This last value is presumed to be an underestimate of the true stoichiometry of one proton for one *myo*-inositol molecule due to some proton exchange for osmotically active species. This hypothesis was confirmed by using SGLT1 as a proton-driven glucose cotransporter. In conclusion, despite the inherent difficulty in estimating the osmotic effect of a proton influx, the volumetric method was found valuable as it has the unique capacity of detecting unidentified transported substrates.

Inositols are neutral cyclic polyols, among which the stereoisomer *myo*-inositol (MI) is by far the most abundant and important in mammalian tissues. MI has many important roles; it is a precursor to phosphatidylinositols (PtdIns) and to the inositol phosphates (IP), which serve as second messengers and as key regulators of many cell functions (Berridge, 1993; Zhang & Majerus, 1998). It is also well established that MI serves as a compatible osmolyte during volume regulation in many tissues where cells are exposed to hyperosmotic conditions (Nakanishi *et al.* 1989; Trachtman, 1992; Wiese *et al.* 1996). MI can also act as a chemical chaperone, assisting in the correct folding of mutant, disfunctional proteins as seen with the ΔF508 deletion in the cystic fibrosis transmembrane conductance regulator (CFTR) protein (Howard *et al.* 2003; Zhang *et al.* 2003). Normal MI levels in serum range from 30 to 70 μM (MacGregor & Matschinsky, 1984; Dolhofer & Wieland, 1987; Kouzuma *et al.* 2001), but can be up to 6 mM in human brain and as much as 17 mM in certain neurones (Fisher *et al.* 2002), as well as 30 mM in outer renal medullary thick ascending limb cells (Schmolke *et al.* 1990). Accumulation of MI within cells against its concentration gradient is accomplished by cotransport, using the electrochemical gradient of the coupled ion.

The cloning of the Na^+/*myo*-inositol cotransporter SMIT1 was achieved more than a decade ago (Kwon *et al.* 1992), and the role played by this cotransporter in cellular adaptation to hypertonicity has been intensively studied (Ibsen & Strange, 1996; Wiese *et al.* 1996; Yamauchi *et al.* 1996). Our laboratory has recently identified a second Na^+/MI cotransporter, named SMIT2 (Coady *et al.* 2002),

which is 43% identical to SMIT1. SMIT1 and SMIT2 are both expressed in the kidney and also in the brain, where they are present both in glial cells and in neurones (Poppe *et al.* 1997). HMIT, a proton-coupled *myo*-inositol transporter, was also recently identified (Uldry *et al.* 2001) and is predominantly expressed in the brain. The precise physiological roles of SMIT2 and HMIT are not known, and the requirement for three distinct, secondary active MI cotransporters (with similar reported affinities for MI) in the brain is not known. Transport stoichiometry (the number of ions cotransported per substrate molecule) is a crucial parameter that can help to rationalize the expression patterns of these cotransporters; stoichiometry sets the energy cost of transport, defining the accumulation capacity of each protein. The exact stoichiometry of each of the three cotransporters remains unknown although the Hill coefficients obtained from the Na^+-activation of SMIT1 and SMIT2 suggest ratios of more than one sodium ion per MI molecule transported (Hager *et al.* 1995; Coady *et al.* 2002).

Several methods exist to establish a transport stoichiometry; they rely on one of the following (i) the ratio between the fluxes of two radiotracers (Kanai *et al.* 1995; Jennings & Adame, 2001); (ii) the ratio between one radiotracer flux and the net flux of electrical charge (Klamo *et al.* 1996; Diez-Sampedro *et al.* 2001); (iii) the thermodynamic equilibrium, by measuring the reversal potential as a function of substrate concentration (Lapointe *et al.* 1986; Smith-Maxwell *et al.* 1990; Chen *et al.* 1995) or by balancing the electrochemical gradients of all transported species in order to reach equilibrium, i.e. the static head method (Turner & Moran, 1982; Fukuhara & Turner, 1984). Here we have employed a novel method based on the fact that cell volume can be measured with high accuracy in oocytes expressing individual forms of transporters. Volume measurements can be used to calculate the total quantity of osmolyte uptake upon stimulation of transport and, when compared with electrophysiological measurements under voltage-clamp conditions, can yield the apparent amount of osmolyte uptake per elementary charge transported. This method is applied here to SMIT2, HMIT and the Na^+/glucose cotransporter (SGLT1), and the results are compared to simultaneous measurements of radiolabelled substrate uptake and cotransport current. The methods confirm a 2 : 1 stoichiometry for SGLT1 and establish the stoichiometries of SMIT2 and HMIT as 2 Na^+ : 1 MI and 1 H^+ : 1 MI, respectively.

Methods

Oocyte preparation and incubation

Stage V–VI *Xenopus laevis* (University of Alberta, Edmonton, Canada) oocytes were surgically removed under tricaine anaesthesia and manually separated. They were then placed into a Ca^{2+}-free buffered saline solution (200 mosmol) and defolliculated by collagenase digestion. The oocytes were maintained at 18°C in Barth's solution (in mm: 90 NaCl, 3 KCl, 0.82 $MgSO_4$, 0.41 $CaCl_2$, 0.33 $Ca(NO_3)_2$, 5 Hepes, pH 7.6) supplemented with 5% horse serum, 2.5 mm sodium pyruvate, 100 U ml^{-1} penicillin and 0.1 mg ml^{-1} streptomycin. All experiments were performed in accordance with the regulations of the Comité de déontologie de l'expérimentation sur les animaux of the Université de Montréal, and following the experiments the frogs were humanely killed.

cRNA preparation and injection

SMIT2 RNA was transcribed from the rabbit cDNA coding region as previously described (Coady *et al.* 2002). *SGLT1* RNA was transcribed from a human cDNA clone (Hediger *et al.* 1989; Bissonnette *et al.* 1999). *HMIT* RNA was transcribed from a cDNA clone in which the sequences coding for endoplasmic reticulum retention and internalization were omitted (Uldry *et al.* 2001) and was kindly provided by Dr B. Thorens (Institute of Pharmacology and Toxicology, Lausanne, Switzerland*),* while aquaporin cDNA clones (AQP1 and AQP2) were kindly provided by J.M. Verbavatz (CEA/Saclay, Gif-sur-Yvette Cedex, France) and D. Bichet (Hôpital du Sacré-Cœur de Montréal, Canada), respectively. Rat renal outer medullary potassium channel (*ROMK2*) cDNA was kindly provided by J. Xu and S.C. Hebert (Yale University, New Haven CT, USA). RNA was injected (46 nl, 0.25 ng nl^{-1} for *SMIT2* and *HMIT*, 0.1 ng nl^{-1} for *SGLT1*) using a Drummond microinjector (Broomall, PA, USA) and oocytes were assayed 5–9 days after injection. *AQP* and *ROMK* RNA (46 nl, 0.1 ng nl^{-1}) were injected 1–2 day before use for volume measurements.

Solutions

Our control solution for both types of experiments contained (in mm): 80 NaCl, 3 KCl, 0.82 $MgCl_2$, 0.74 $CaCl_2$ and 25 mannitol. For SGLT1 and SMIT2, solutions were buffered with 5 mm Hepes, pH 7.6 titrated with NaOH. For HMIT we used 10 mm mes titrated with Tris to pH 6.0 or 5.5 as indicated. Solutions containing alpha-methyl-D-glucopyranose (αMG, a non-metabolized substrate for SGLT1) or *myo*-inositol were obtained by replacing 1, 5 or 10 mm of mannitol by the appropriate substrate, and hyposmotic solutions were made by omitting 20 mm mannitol. For Na^+-free solutions used with SGLT1 as a H^+-driven cotransporter, NaCl was omitted and replaced by 45 mm NMDG titrated to pH 7.0 with HCl, and 100 mm mannitol or αMG. The solution final pH of 5.5 was reached by adding 10 mm mes and the appropriate amount of Tris. For ROMK2, KCl was increased to 20 mm KCl in order to activate the channel and sodium was commensurately diminished. Phloridzin (Pz), an inhibitor of MI and

αMG transport, was used for stop and rinse solutions for radioactive uptake experiments; these were made daily by directly dissolving Pz in the control solution. Measured osmolalities were $\sim$197 mosmol (kg H_2O)$^{-1}$ for control and substrate solutions and $\sim$177 mosmol (kg H_2O)$^{-1}$ for hyposmotic solution, their difference always being 20 mosmol (kg H_2O)$^{-1}$, and osmolalities were verified within $\pm$2 mosmol (kg H_2O)$^{-1}$ using a freezing-point osmometer (Advanced DigiMatic Osmometer, model 3D2, Advanced Instruments, Needham Heights, MA, USA).

Volume measurements

The apparatus used for volumetric measurements has previously been described (Gagnon *et al.* 2004). Briefly, a chamber of 120 μl is illuminated from above by a light-emitting diode touching the surface of the solution. It was perfused, at a rate of $\sim$1.5 ml min^{-1}, under the control of an electrical valve with a characteristic dead space of 50 μl. The oocyte cross-section was continuously measured from below with a CCD camera and a 3$\times$ objective. Custom-made software was used to count the number of pixels corresponding to the oocyte cross-section five times per second, and data were later averaged over 1 s periods. Oocyte volume was obtained assuming spherical symmetry and calibrating with a steel ball of known volume. After allowing a stabilization period of at least 20 min, a noise level for volume measurements of 0.05% could usually be obtained.

Electrophysiology

For simultaneous current and volume measurements, the two-electrode voltage-clamp technique previously described in our laboratory was used (Duquette *et al.* 2001; Gagnon *et al.* 2004). Voltage-sensing electrodes were filled with 1 M KCl as described, but current-injecting electrodes were filled with a unique solution (in mM: 10 NaCl, 15 KCl, 70 K-gluconate, 10 Hepes pH 7.4). This was done to minimize salt exchange between electrode and cytosol, and to reduce Cl$^-$ injection when cotransporter activation generated an inward current. Current data acquisition was performed with Fetchex 6 (Axon Instruments, Union City, CA, USA) at a sampling rate of 40 Hz, and analysis was made using Matlab 5.3 (MathWorks, Inc., Natick, MA, USA). The bath reference and current electrodes were Ag–AgCl pellets. The chamber was continuously perfused with control saline. Oocytes expressing cotransporters were maintained at $-$50 mV. For experiments with ROMK, the resting potential was measured for each oocyte ($\sim$$-$35 mV with 20 mM extracellular K$^+$) and the membrane potential was later clamped a few millivolts more negative to generate an inward potassium current between 0.5 and 2 μA.

Radiotracer experiments

For experiments comparing current and radiotracer uptake, both electrodes contained 1 M KCl. A non-perfused chamber of $\sim$1200 μl was used. The oocytes were initially impaled and clamped at $-$50 mV in 400 μl of control solution. When a stable baseline was reached, 400 μl of solution containing twice the desired concentration of substrate and radiolabelled substrate (1 μCi μl^{-1} [2-^{3}H]MI or 0.1 μCi μl^{-1} [glucose-^{14}C(U)] αMG) was gently added to stimulate a cotransport current. After 10–15 min of transport, 400 μl of saline solution containing 2 mM phloridzin was added as a stop solution to inhibit further transport and current. Electrodes were carefully withdrawn from the oocyte, which was then removed from the bath and rinsed 3–4 times in a saline solution containing 667 μM phloridzin before being transferred to a scintillation vial and dissolved in 200 μl 10% SDS for at least 2 h; 5 ml scintillation cocktail (Beta Blend; ICN, Irvine, CA, USA) was then added and the vials were assayed for ^{3}H or ^{14}C activity with an LS6000 SC scintillation counter (Beckman, Fullerton, CA, USA). During the transport experiment, 20 μl of bathing medium was removed from the bath and radioactivity was assayed in the same manner in order to calculate the total quantity of substrate that entered the oocyte. Substrate concentrations used in the bath were between 500 and 2500 μM for SGLT1, SMIT2 and HMIT (for which the pH was set at 5.5). Control oocytes (non-injected) were exposed to the same treatment, with either radiolabelled αMG or *myo*-inositol. Transport activity into control oocytes was negligible for both substrates.

Concomitant transport current

Net flux of cotransported charge is obtained by integrating the total current minus baseline over time as linearly interpolated between the current before addition of substrate and after specific inhibition. As the initial baseline includes a leak current which is not present after transport inhibition, this calculation leads to a certain underestimation of transferred charge; however, as the leak current is often smaller than the spontaneous changes in the baseline current over time, correction for the leak current was not employed in the present study.

Volumetric method

Water permeability (P_f) of individual oocytes was calculated from the swelling induced by a hyposmotic shock according to the following relation:

$$P_f = \frac{1}{S \times v_w \times \Delta\pi}\left(\frac{dV}{dt} - \frac{dV}{dt_0}\right) \qquad (1)$$

where $dV/dt - dV/dt_0$ is the difference in water fluxes, in this case measured immediately after and immediately

before the shock, respectively. v_w is the specific volume of water ($18.2\,cm^3\,mol^{-1}$), $\Delta\pi$ is the size of the hyposmotic shock imposed and S is a standard oocyte surface of $0.4\,cm^2$ assuming a membrane infolding factor of about 9 (Zampighi *et al.* 1995).

As AQP was coexpressed with each of the different cotransporters, isosmoticity of transport is rapidly achieved as shown by the fact that the swelling rate
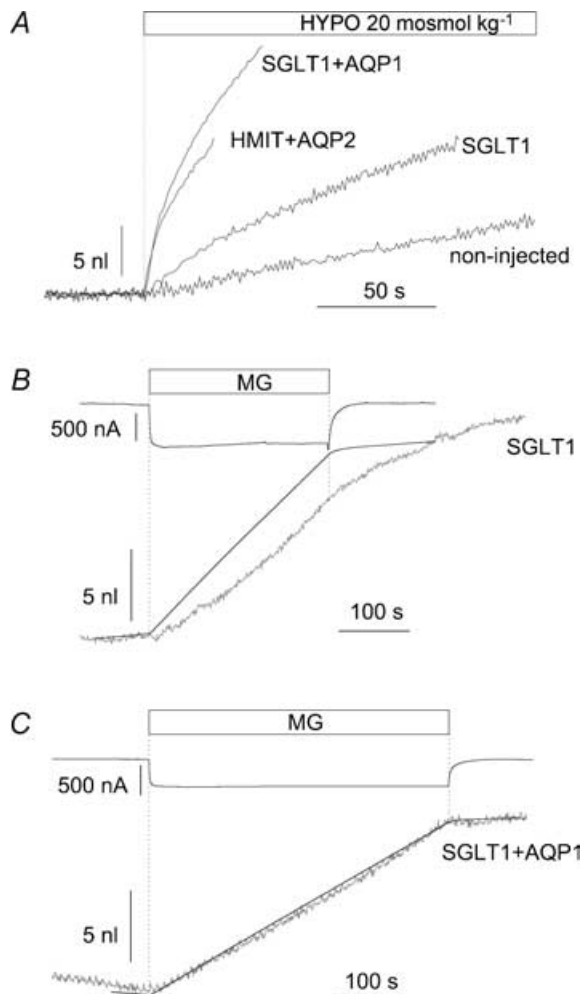

Figure 1. Aquaporin effects
A, volume response to a 20 mosmol hyposmotic shock by a control oocyte or by oocytes expressing different cotransporters and water channels. In these examples, the measured water permeabilities were $3.4\,\mu m\,s^{-1}$ for the non-injected oocyte and 11, 79 and 87 $\mu m\,s^{-1}$ for oocytes expressing SGLT1, HMIT + AQP2 and SGLT1 + AQP1, respectively. *B*, volume response to the addition of 5 mM α-methylglucose (αMG) for oocytes expressing SGLT1. The continuous line is the volume predicted from current integration assuming an isosmotic swelling, using the solution osmolarity and the best apparent osmolytes per charge (n_{OPC}). In the absence of AQP1, the cotransport stimulation induces a swelling that continues after substrate removal, indicating a net increase in intracellular osmolyte concentration during the transport period. *C*, when AQP1 is present, swelling ceases immediately after the substrate is removed, indicating that isosmotic transport is achieved.

reaches a constant value shortly after the addition of a cotransported substrate (see Fig. 1*C* for an example). Under these conditions, the net rate of osmolyte uptake (R_O) can be obtained from the relation:

$$R_O = \pi \left(\frac{dV}{dt} - \frac{dV}{dt_0} \right) \quad (2)$$

where π is the osmolarity of the bathing medium and dV/dt and dV/dt_0 refers to water fluxes during and before cotransport, respectively. Note that the specific pathway used by water to cross the oocyte membrane is irrelevant here provided that the net influx is assumed to be isosmotic. The concomitant rate of charge uptake (R_C), in moles of elementary charge per second, can be easily obtained by dividing the cotransport-associated membrane current measured over the same time interval by the Faraday constant:

$$R_C = \frac{\langle I - I_0 \rangle}{F} \quad (3)$$

The ratio of the two preceding quantities yields the apparent number of osmolytes taken up per charge (n_{OPC}):

$$n_{OPC} \equiv \frac{R_O}{R_C}$$

At this point it is important to underscore the difference between n_{OPC} and true stoichiometry. n_{OPC} includes ionic movement that takes place at the electrode in order to maintain the membrane potential. For example, the apparent number of osmolytes per charge for a purely monovalent cationic transport across the membrane can be tested by analysing potassium influx through ROMK2. It corresponds to one osmolyte per charge for each K^+ ion entering the cell minus OA_e, the average number of osmolytes absorbed by the current electrode for each electrical charge injected:

$$n_{OPC}(K^+ \text{ influx}) = 1 - OA_e \quad (4)$$

$n_{OPC}(K^+$ influx) could then vary between 0 and 2, depending on the process occurring at the current electrode to compensate for K^+ influx through the channel. For example, it would be 0 if intracellular K^+ ions were absorbed by the current electrode and it would be 2 if the electrode was injecting a negative ion for each charge entering the cell. For cotransport of x neutral substrates per cation, the apparent number of osmolytes per charge transported is given by simply adding x to the right hand side of eqn (4):

$$n_{OPC}(\text{cotransport}) = 1 + x - OA_e \quad (5)$$

After measuring the n_{OPC} values both for cotransport (eqn (5)) and for a pure cationic flux (eqn (4)), x for a given cotransporter can be calculated as follows:

$$x = n_{OPC}(\text{cotransport}) - n_{OPC}(K^+ \text{ influx}) \quad (6)$$

The stoichiometry is simply $1/x$, the number of cations per substrate molecule transported.

In the case of HMIT, a proton influx cannot be treated like a Na^+ or a K^+ influx with regard to the osmotic effect produced. Considering that the *Xenopus* oocyte buffering power has been estimated at 23.8 mM per pH unit at physiological pH (Sasaki *et al.* 1992), it can be calculated that fewer than one proton out of 10^5 entering an oocyte will remain unbound. Thus, our working hypothesis is that proton influx does not generate new intracellular osmolytes and that the apparent number of transported osmolytes per charge for HMIT would be given by:

$$n_{OPC}(H^+ \text{ cotransport}) = 0 + x - OA_e \qquad (7)$$

As electrodes behave independently of the type of charge cotransported, the same OA_e applies, and x can be found from eqn (7) – eqn (4)

$$x = n_{OPC}(H^+ \text{ cotransport}) - \left[n_{OPC}(K^+ \text{ influx}) - 1 \right] \qquad (8)$$

Results

Aquaporin expression and isosmotic transport assumption

Figure 1*A* shows the volume change triggered by a hyposmotic shock for oocytes expressing different transporters. As previously reported (Loo *et al.* 1999; Duquette *et al.* 2001), the presence of SGLT1 increased the oocyte P_f by a factor of 2 (see Fig. 1*A*). Oocytes expressing HMIT or SMIT2 alone displayed water permeabilities very similar to the permeabilities observed with SGLT1 (data not shown). As illustrated in Fig. 1*A*, the presence of either AQP1 or AQP2 stimulated the oocyte P_f by at least an order of magnitude. Fig. 1*B* and *C* shows the impact of this enhanced water permeability on transport-induced swelling. In the absence of AQP1 (*B*), at least 2 min are required for the cotransport-associated cell swelling to reach a constant value that parallels the uptake of Na^+ and αMG (shown here as the integral of the cotransport current). Not surprisingly, when cotransport current is shut down by removing αMG, the cell continues to swell for a few minutes before reaching a stable level. In contrast, in the presence of AQP1 (see Fig. 1*C*), the cell swelling closely follows the volume predicted by the integral of the cotransport current and quickly stops upon removal of substrate. This is fully consistent with isosmotic influx of water and osmolytes during the transport period.

Osmolyte uptake and cation influx

In Fig. 2, the combined effects of cation influx across the membrane and compensating current injection through the current electrode are shown using an oocyte expressing

ROMK2 and AQP1. In the example presented, an inward K^+ flux corresponding to a 680 nA current was elicited by clamping the membrane potential a few millivolts more negative than the equilibrium potential. A difference of 22 pl s^{-1} in the oocyte swelling rate was immediately recorded. If the transport-dependent influx is assumed to be isosmotic with respect to the bathing solution (192 mosmol), it would correspond to an osmolyte uptake rate of 4.2 pmol s^{-1}. As the observed K^+ current corresponded to 7.0 pmol s^{-1}, this represents a ratio of 0.6 apparent osmolytes per charge. The average apparent amount of osmolytes per charge obtained for a series of similar ROMK2 experiments ($n_{OPC}(K^+$ influx$)$) was 0.46 ± 0.07 (mean ± S.E.M., $n = 15$).

Cotransport-induced swelling

Volume and current were recorded from oocytes expressing SMIT2, SGLT1 and HMIT with either AQP1 or AQP2 (the use of two different aquaporins is explained in the Discussion). Examples of volume increases are presented in Fig. 3, together with associated clamp currents for the three cotransporters. In each case, it can be seen that the isosmotic swelling assumption is clearly supported since a constant transport rate induced a linear swelling rate, as well as because the oocyte volume rapidly reached a stable volume when cotransport was abruptly stopped. By analysing the volume and current measurements as described in the Methods section, the n_{OPC} was determined for each transporter: 1.02 ± 0.04 osmolyte $(Na^+)^{-1}$ ($n = 14$) for SGLT1, 1.03 ± 0.06 osmolyte $(Na^+)^{-1}$ ($n = 9$) for SMIT2 and 0.96 ± 0.08 osmolyte $(\text{proton})^{-1}$ ($n = 10$) for HMIT.
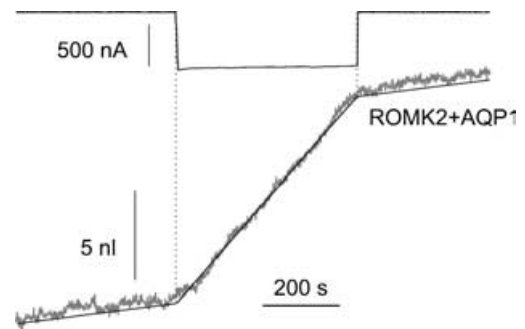

Figure 2. Simultaneous volume and current measurements in an oocyte expressing ROMK2 and AQP1
Current and volume were monitored in a 20 mM [K^+] solution as the membrane potential was suddenly clamped ~1 mV more negative than the K^+ equilibrium potential. The inward current immediately triggered a volume uptake that was used to calculate the apparent amount of osmolyte transported for each K^+ ion entering the oocyte. The continuous line is the volume predicted if the swelling is assumed to be isosmotic with $n_{OPC} = 0.6$.

Stoichiometry calculation and accuracy

The number of electrical charges per substrate molecule transported can be readily obtained from the volumetric experiments as $1/x$ by using eqn (6) or eqn (8). As the stoichiometry (S) is derived as the inverse of a difference in n_{OPC}, an underestimate in a particular n_{OPC}(cotransport) measurement could lead to a very high stoichiometric ratio which would skew the average ratio toward higher values. We chose to avoid this by obtaining an average n_{OPC} with a s.e.m. value for each cotransporter, and using this value to derive the stoichiometry. In the case of Na$^+$ cotransport (Fig. 4A), the stoichiometric scale, as the number of charges per neutral osmolyte transported, was

Figure 3. Simultaneous volume and current measurements in oocytes expressing SGLT1 and AQP1 (*A*), SMIT2 and AQP1 (*B*), or HMIT and AQP2 (*C*)
Isosmotic addition of *myo*-inositol (MI) or α-methylglucose (αMG) (5 mM, 1 mM and 10 mM, respectively) to oocytes clamped at -50 mV elicited inward currents together with linear swelling due to influx of both ions and substrates. Broken lines present volume prediction from current integration for best n_{OPC} fit and for this $n_{OPC} \pm 0.2$. The time and volume scales apply to all three panels.

obtained from eqn (6):

$$S = \frac{1}{x} = \frac{1}{n_{OPC}(\text{cotransport}) - n_{OPC}(\text{K}^+ \text{ influx})}$$

(9)

As expected, as n_{OPC}(cotransport) approaches n_{OPC}(K$^+$ influx), the number of substrate transported per Na approaches 0 and S approaches ∞. The same applies for H$^+$ cotransport (Fig. 4B), with the stoichiometric scale obtained from eqn (8):

$$S = \frac{1}{x} = \frac{1}{n_{OPC}(\text{H}^+ \text{ cotransport}) - [n_{OPC}(\text{K}^+ \text{ influx}) - 1]}$$

(10)

It should be noted that the errors associated with an over- or underestimation of n_{OPC} are not symmetrical. If one considers the differences between n_{OPC}(cotransport) and n_{OPC}(K$^+$ influx) and computes the errors by standard rules of error propagation (for a difference: $\sigma_{diff}^2 = \sigma_a^2 + \sigma_b^2$), and then observes the effect of a variation on each difference by 1 s.e.m., different error values will be obtained toward positive or negative values, yielding a two-part error. Consequently, the stoichiometries obtained here (net charge per substrate molecule transported) are most accurately described as $1.78 + 0.31 - 0.23$ for SGLT1 and $1.75 + 0.35 - 0.25$ for SMIT2. In the case of HMIT, as it is assumed that the protons are osmotically invisible, the stoichiometry calculated is $0.667 + 0.052 - 0.045$ net charges per substrate molecule transported. For the sake of comprehensibility, the two errors were averaged, producing the following values: 1.78 ± 0.27 for SGLT1, 1.75 ± 0.30 for SMIT2 and 0.67 ± 0.05 for HMIT.

H$^+$ cotransport with SGLT1

As a test of validity for the hypothesis that entering protons are osmotically invisible, we measured the swelling induced by SGLT1 activity when working as a proton-driven glucose cotransporter with a known stoichiometry of 2 : 1 (Quick *et al.* 2001). The transport-dependent steady-state swelling rates measured yielded an average n_{OPC} of 0.33 ± 0.11 (Fig. 4B, $n = 5$) suggesting a stoichiometry of 1.41 ± 0.17 : 1. This indicates that protons are not totally osmotically invisible.

Radiolabelled substrate uptake

Voltage-clamped oocytes were exposed to radiolabelled substrate (^{3}H-MI or ^{14}C-αMG) for a period of at least 10 min as explained in the Methods section. The relationships between the net transported charge and the substrate influx are presented in Fig. 5 for SGLT1, SMIT2 and HMIT. As the cotransport currents and
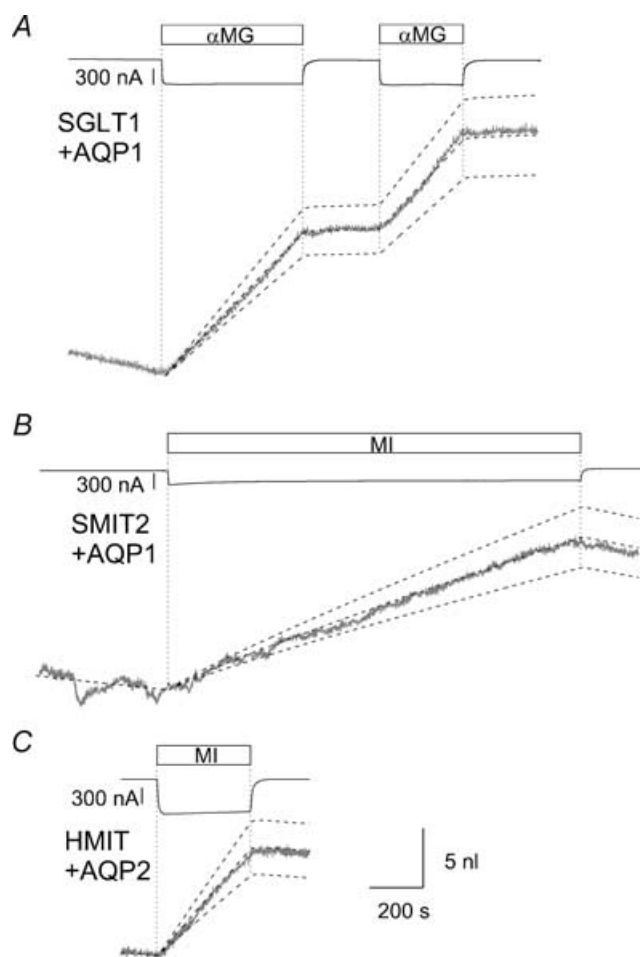
the substrate uptakes were not significantly different from zero for non-injected oocytes (O), each experiment performed with an injected oocyte can be considered as an independent determination of the cotransporter stoichiometry. The average ± s.e.m. values of these independent determinations yield cation to substrate stoichiometries of 2.14 ± 0.05 for SGLT1 ($n = 10$), 1.82 ± 0.10 for SMIT2 ($n = 9$) and 1.03 ± 0.04 for HMIT ($n = 16$).

Discussion

Several methods exist for determining cotransporter stoichiometry, demonstrating variable degrees of ease and accuracy. The determination of Hill numbers for cation or substrate-activated cotransport is an easily accessible method but it only provides a measure of the degree of cooperativity in the binding process (Weiss, 1997). In other words, this analysis can suggest that more than one molecule appears to interact but it is by no mean an accurate determination of the actual stoichiometry. The thermodynamic method, using the reversal potential of a cotransport-specific current, can distinguish between a substrate that is interacting with the cotransporter and a substrate that is actually transported across the membrane (Chen *et al.* 1995; Gross & Hopfer, 1996). It obviously requires an electrogenic transport process, whose reversal potential has to be in the measurable voltage range. In the case of SMIT2, this method could not be used as the cotransporter is strongly rectifying (unpublished results), which makes the determination of the reversal potential

inaccurate. The simultaneous measurement of a current and a radiolabelled substrate transport rate is appropriate when the background transport rate and binding are negligible, but it requires dedication of an electrophysiological setup to the use of radioisotopes. In the present study, we examined the possibility of measuring oocyte volumes with high accuracy as an innovative method of measuring cotransport stoichiometry. The method was tested successfully with the high-affinity Na^+/glucose cotransporter (SGLT1) before applying it to two MI cotransporters of unknown stoichiometry.

The number of osmolytes per charge (n_{OPC}) for a pure K^+ current

The measured stoichiometry values are based on the determination of n_{OPC}, which reflects the number of osmolytes accompanying a transported charge at the plasma membrane minus the number of osmolytes withdrawn from the cell by the current electrode. A theoretical estimate can be derived for the electrode performance by considering the fraction of the current carried by each ion present, as given by its transport number:

$$t_i = \frac{z_i^2 u_i C_i}{\sum_j z_j^2 u_j C_j} \tag{11}$$

where z_i is the valence of the ion 'i', C_i is its concentration and u_i, its mobility. The solution present at the tip of the electrode after being inserted into the oocyte for several minutes is expected to be a mixture between the cytosol
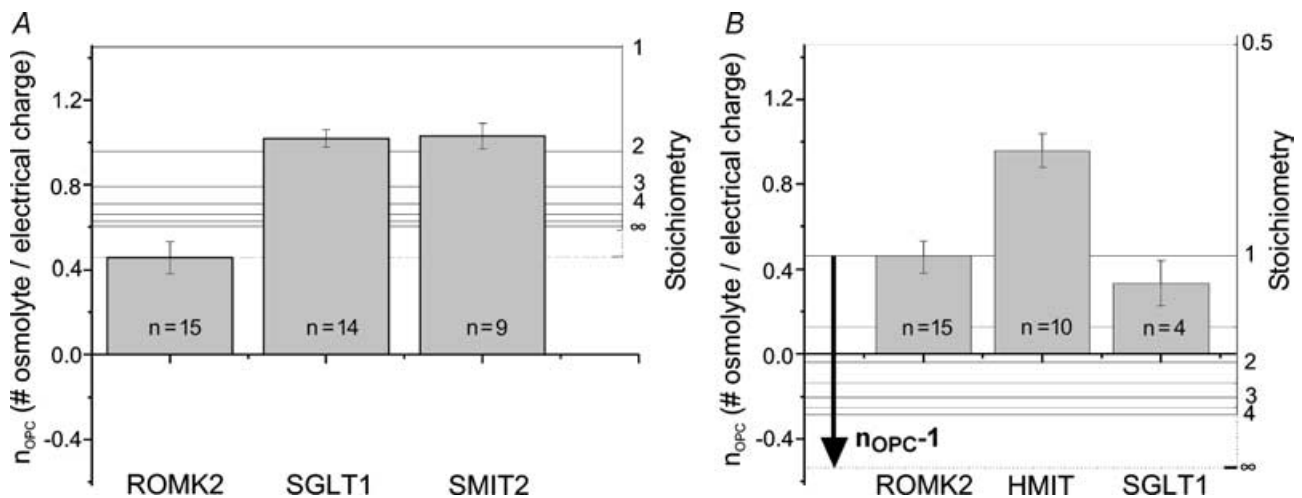

Figure 4. Stoichiometry and apparent osmolyte influx per charge transported for the potassium channel and for transporters
The left scale shows the apparent number of osmolytes measured per charge (n_{OPC}), while the right scale indicates the corresponding stoichiometry according to eqn (9) or eqn (10). *A*, Na^+ : substrate stoichiometry for sodium cotransport; *B*, H^+ : substrate stoichiometry for proton cotransport. Stoichiometric values for proton cotransport are calculated from n_{OPC}(K^+ influx) values reduced by 1 due to the hypothesized osmotic invisibility of protons (see eqn (10), Methods).

and the intracellular pipette solution; these differ mainly in the major anions present. At the electrode tip, if the ionic composition is dominated by the pipette solution (including 70 mM gluconate with a relative mobility to K^+ of 0.33), the transport number for all cations 't^+' would be 0.65. In the case of K^+ influx through ROMK2, this means that for each K^+ ion entering the cell, 0.65 cations are leaving and 0.35 anions are entering at the current electrode, yielding a n_{OPC} value of 0.70. On the other hand, if the solution at the electrode tip is similar to the cytosol with large, poorly mobile anions and a K^+ concentration of 100 mM, t^+ can be estimated at 0.78, yielding a $n_{OPC}(K^+$ influx) value of 0.44. The experimentally measured n_{OPC}

Figure 5. Correlation between substrate-dependent net charge influx and radiolabelled substrate influx

Each point corresponds to a different oocyte; ○ represents six non-injected oocytes tested with ^{14}C-α-methylglucose or four injected with ^{3}H-*myo*-inositol, and all are positioned near the origin. Results were fitted to a straight line going through the origin for SGLT1, SMIT2 and HMIT (upper, centre and lower panel, respectively). Inset: typical current trace recorded during addition of 2.5 mM MI followed by inhibition of cotransport with 667 μM Pz.

(0.46) is thus consistent with a situation where the conduction at the tip of the current electrode is dominated by the cations present.

Interpretation of the stoichiometry numbers obtained

We confirmed the 2 : 1 stoichiometry of SGLT1 (previously established by several techniques) and determined stoichiometry for SMIT2 and HMIT by two distinct methods, both directly by comparing sugar-dependent currents and radiolabelled sugar uptake in the same oocyte, and indirectly by measuring oocyte swelling due to osmolyte uptake and comparing it to the clamp current. Overexpression of the transporters minimizes the importance of non-specific substrate fluxes, either by passive diffusion or by other transporters. For SGLT1, we obtained stoichiometry values of 2 Na^+ : 1 αMG with both the direct method and with the swelling method, validating our methodology since the SGLT1 stoichiometry was previously established at 2 Na^+ : 1 αMG by different methods (Chen *et al.* 1995; Mackenzie *et al.* 1998). In the case of SMIT2, both the volumetric and the radiotracer methods yielded a stoichiometry of 2 Na^+ : 1 MI. This is in agreement with the Hill number of 1.4 reported for the Na^+ activation of SMIT2 (Coady *et al.* 2002). Due to low expression levels in oocytes, the stoichiometry for SMIT1 has not yet been evaluated. However, the Hill number obtained for the Na^+ activation of SMIT1 is 1.9 (Hager *et al.* 1995), suggesting that more than 1 Na^+ ion is involved in the MI cotransport. Therefore, different stoichiometries cannot be used to rationalize the presence of two distinct Na^+/MI cotransporters found in the same organ (Kwon *et al.* 1992; Poppe *et al.* 1997). The reasons for having two Na^+/MI cotransporters of similar stoichiometry may well be related to specific types of regulation and/or to different subcellular expression patterns (e.g. apical *versus* basolateral membrane.)

HMIT

Two different homologues of aquaporin water channels were used in our experiment. With its high water permeability and good expression in *Xenopus* oocytes, AQP1 performed perfectly in experiments involving SGLT1 and SMIT2. However, when extracellular pH was decreased to 5.5 during experiments with HMIT, abnormal currents of many hundred nanoamperes were recorded upon addition of substrate, when AQP1 was either expressed alone or coinjected with HMIT (data not shown). The purported ion channel activities of AQP1 have been a matter of debate in recent years (Yool *et al.* 1996; Anthony *et al.* 2000; Saparov *et al.* 2001; Tsunoda *et al.* 2004), although we have not found any claims of pH dependency. Nonetheless, we turned to AQP2 for coexpression with HMIT. We found that AQP2 had similar
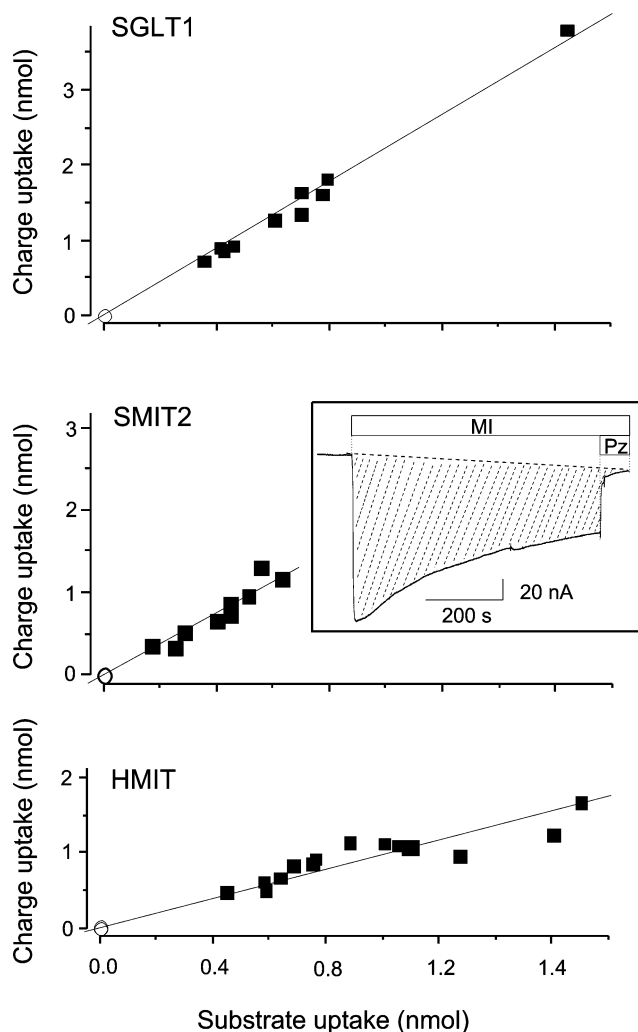
levels of activity to those of AQP1, but exhibited no abnormal currents in acidic conditions.

An apparent discrepancy seems to exist in our measurements of HMIT stoichiometry. While the direct method yields a proton : MI stoichiometry of 1 : 1, the swelling method gives a charge to neutral osmolytes ratio of only 0.67 ± 0.05 suggesting that more than one MI is transported per proton. This possibility is unlikely as the activation of HMIT by MI follows an unmodified Michaelis–Menten equation, i.e. it is strictly hyperbolic with respect to MI concentration. It is also unlikely that another neutral substrate accompanies MI in the cotransport process as, with the exception of mannitol, there was no other neutral molecule in any of our experimental solutions. The possibility that Cl^- could be associated with the cotransport has also been tested, but varying the extracellular Cl^- concentration did not affect the MI-stimulated cotransport current (data not shown). Another possibility is that proton uptake might not be completely osmotically inactive. The observed $n_{OPC}(H^+$ cotransport) would be consistent with a stoichiometry of 1.00 ± 0.11 protons per MI if it is assumed that one half of the protons transported become osmotically visible instead of being simply captured by intracellular buffers. This could happen if the activation of oocyte pH regulatory mechanisms resulted in replacing a fraction of the transported protons by an osmotically active species. For example, a sodium/proton exchanger which is endogenously present in *Xenopus laevis* oocytes (Burckhardt *et al.* 1992) could be responsible for this phenomenon. Indeed, if the entry of protons mediated by HMIT activates the $Na^+ : H$ exchanger, some of the recently transported intracellular protons would be replaced by Na^+ and would be detected as active intracellular osmolytes instead of being captured by intracellular buffer. However, no change in swelling rate was observed when amiloride was added (data not shown), suggesting that a transport mechanism different from the $Na^+ : H$ exchanger, or some other intracellular chemical reactions could be involved in exchanging protons for osmotically active species.

The hypothesis that entering protons are not completely buffered is supported by the n_{OPC} measured when SGLT1 is used as a proton-driven glucose cotransporter. A stoichiometry of 1.14 ± 0.17 protons per glucose is calculated if protons are assumed to be completely buffered, but this stoichiometry would reach 2.6 ± 1.0 if half of the entering protons end up being osmotically active. Inversely, if the stoichoimetry scale of Fig. 4*B* is adjusted to give two protons per glucose transported as previously measured for SGLT1 (Quick *et al.* 2001), the stoichiometry for HMIT would increase to 0.89 ± 0.11 $H^+ : 1$ MI which would be in excellent agreement with the value found using the radioactive uptake method.

HMIT acts in a very different manner from SMIT1 and SMIT2; not only does it use protons and have a much lower affinity for MI (despite the previously published value of $100 \mu M$ (Uldry *et al.* 2001), in our hands the K_m for MI was ~ 6 mm, data not shown), but its 1 : 1 stoichiometry dictates a lower concentration capacity for a given ionic gradient. The brain is the principal location of HMIT. Mammalian brain cells are typically maintained at a pH about 7.0–7.2 for an external pH of 7.3, so the Nernst potential for protons must be between -10 and -20 mV; an inward electromotive force of about 50 mV thus exists for protons, which could account for an intracellular MI accumulation 10 times the extracellular concentration. The MI concentrations in neurones were reported to be as high as 10 mm for a cerebrospinal fluid concentration of $470 \mu M$ (Spector & Lorenzo, 1975; Fisher *et al.* 2002). A possible role of HMIT in maintaining such a MI gradient remains to be established as, at least in oocytes, HMIT requires an acidic extracellular medium to become really active. The recent localization and regulation of HMIT at sites of extracellular medium acidification would satisfy this requirement (Chesler & Kaila, 1992; Uldry *et al.* 2004).

Volumetric method

The volumetric method used to determine stoichiometry presents a certain number of advantages with respect to other published methods. First, it does not require the use of radioactive labelled substrates, which are not always commercially available. Second, it allows for the detection of all transported and osmotically active species. This could be helpful in distinguishing between ions or solutes that interact with a transporter either without crossing the membrane or in exchange for another, identical ion (as in the case for Cl^- in gamma-aminobutyric acid transporters (Loo *et al.* 2000; Sacher *et al.* 2002). It can also help in identifying all of the substrates involved in complex cotransporter and exchange mechanisms. Despite these interesting advantages, one caveat must be borne in mind: since the stoichiometry is provided by the inverse of a difference in n_{OPC} values (see eqn (6)), the method is capable of distinguishing between a stoichiometry of 1 : 1 *versus* 2 : 1 (number of charges per substrate transported) but the sensitivity decreases rapidly for stoichiometries of 3 : 1 and higher (see Fig. 4).

References

Anthony TL, Brooks HL, Boassa D, Leonov S, Yanochko GM, Regan JW *et al.* (2000). Cloned human aquaporin-1 is a cyclic GMP-gated ion channel. *Mol Pharmacol* **57**, 576–588.

Berridge MJ (1993). Inositol trisphosphate and calcium signalling. *Nature* **361**, 315–325.

Bissonnette P, Noel J, Coady MJ & Lapointe JY (1999). Functional expression of tagged human Na^+-glucose cotransporter in *Xenopus laevis* oocytes. *J Physiol* **520**, 359–371.

Burckhardt BC, Kroll B & Fromter E (1992). Proton transport mechanism in the cell membrane of *Xenopus laevis* oocytes. *Pflugers Arch* **420**, 78–82.

Chen XZ, Coady MJ, Jackson F, Berteloot A & Lapointe JY (1995). Thermodynamic determination of the Na⁺: glucose coupling ratio for the human SGLT1 cotransporter. *Biophys J* **69**, 2405–2414.

Chesler M & Kaila K (1992). Modulation of pH by neuronal activity. *Trends Neurosci* **15**, 396–402.

Coady MJ, Wallendorff B, Gagnon DG & Lapointe JY (2002). Identification of a novel Na⁺/myo-inositol cotransporter. *J Biol Chem* **277**, 35219–35224.

Diez-Sampedro A, Eskandari S, Wright EM & Hirayama BA (2001). Na⁺-to-sugar stoichiometry of SGLT3. *Am J Physiol Renal Physiol* **280**, F278–F282.

Dolhofer R & Wieland OH (1987). Enzymatic assay of myo-inositol in serum. *J Clin Chem Clin Biochem* **25**, 733–736.

Duquette PP, Bissonnette P & Lapointe JY (2001). Local osmotic gradients drive the water flux associated with Na⁺/glucose cotransport. *Proc Natl Acad Sci U S A* **98**, 3796–3801.

Fisher SK, Novak JE & Agranoff BW (2002). Inositol and higher inositol phosphates in neural tissues: homeostasis, metabolism and functional significance. *J Neurochem* **82**, 736–754.

Fukuhara Y & Turner RJ (1984). The static head method for determining the charge stoichiometry of coupled transport systems. Applications to the sodium-coupled D-glucose transporters of the renal proximal tubule. *Biochim Biophys Acta* **770**, 73–78.

Gagnon MP, Bissonnette P, Deslandes LM, Wallendorff B & Lapointe JY (2004). Glucose accumulation can account for the initial water flux triggered by Na⁺/glucose cotransport. *Biophys J* **86**, 125–133.

Gross E & Hopfer U (1996). Activity and stoichiometry of Na⁺: HCO3⁻ cotransport in immortalized renal proximal tubule cells. *J Membr Biol* **152**, 245–252.

Hager K, Hazama A, Kwon HM, Loo DD, Handler JS & Wright EM (1995). Kinetics and specificity of the renal Na⁺/myo-inositol cotransporter expressed in *Xenopus* oocytes. *J Membr Biol* **143**, 103–113.

Hediger MA, Turk E & Wright EM (1989). Homology of the human intestinal Na⁺/glucose and *Escherichia coli* Na⁺/proline cotransporters. *Proc Natl Acad Sci U S A* **86**, 5748–5752.

Howard M, Fischer H, Roux J, Santos BC, Gullans SR, Yancey PH *et al*. (2003). Mammalian osmolytes and S-nitrosoglutathione promote Delta F508 cystic fibrosis transmembrane conductance regulator (CFTR) protein maturation and function. *J Biol Chem* **278**, 35159–35167.

Ibsen L & Strange K (1996). In situ localization and osmotic regulation of the Na (+) -myo-inositol cotransporter in rat brain. *Am J Physiol Renal Physiol* **271**, F877–F885.

Jennings ML & Adame MF (2001). Direct estimate of 1 : 1 stoichiometry of K⁺–Cl⁻ cotransport in rabbit erythrocytes. *Am J Physiol Cell Physiol* **281**, C825–C832.

Kanai Y, Nussberger S, Romero MF, Boron WF, Hebert SC & Hediger MA (1995). Electrogenic properties of the epithelial and neuronal high affinity glutamate transporter. *J Biol Chem* **270**, 16561–16568.

Klamo EM, Drew ME, Landfear SM & Kavanaugh MP (1996). Kinetics and stoichiometry of a proton/myo-inositol cotransporter. *J Biol Chem* **271**, 14937–14943.

Kouzuma T, Takahashi M, Endoh T, Kaneko R, Ura N, Shimamoto K *et al*. (2001). An enzymatic cycling method for the measurement of myo-inositol in biological samples. *Clin Chim Acta* **312**, 143–151.

Kwon HM, Yamauchi A, Uchida S, Preston AS, Garcia-Perez A, Burg MB *et al*. (1992). Cloning of the cDNa for a Na⁺/myo-inositol cotransporter, a hypertonicity stress protein. *J Biol Chem* **267**, 6297–6301.

Lapointe JY, Hudson RL & Schultz SG (1986). Current-voltage relations of sodium-coupled sugar transport across the apical membrane of *Necturus* small intestine. *J Membr Biol* **93**, 205–219.

Loo DDF, Eskandari S, Boorer KJ, Sarkar HK & Wright EM (2000). Role of Cl⁻ in electrogenic Na⁺-coupled cotransporters GAT1 and SGLT1. *J Biol Chem* **275**, 37414–37422.

Loo DD, Hirayama BA, Meinild AK, Chandy G, Zeuthen T & Wright EM (1999). Passive water and ion transport by cotransporters. *J Physiol* **518**, 195–202.

MacGregor LC & Matschinsky FM (1984). An enzymatic fluorimetric assay for myo-inositol. *Anal Biochem* **141**, 382–389.

Mackenzie B, Loo DD & Wright EM (1998). Relationships between Na⁺/glucose cotransporter (SGLT1) currents and fluxes. *J Membr Biol* **162**, 101–106.

Nakanishi T, Turner RJ & Burg MB (1989). Osmoregulatory changes in myo-inositol transport by renal cells. *Proc Natl Acad Sci U S A* **86**, 6002–6006.

Poppe R, Karbach U, Gambaryan S, Wiesinger H, Lutzenburg M, Kraemer M *et al*. (1997). Expression of the Na⁺–D-glucose cotransporter SGLT1 in neurons. *J Neurochem* **69**, 84–94.

Quick M, Loo DDF & Wright EM (2001). Neutralization of a conserved amino acid residue in the human Na⁺/glucose transporter (hSGLT1) generates a glucose-gated H⁺ channel. *J Biol Chem* **276**, 1728–1734.

Sacher A, Nelson N, Ogi JT, Wright EM, Loo DD & Eskandari S (2002). Presteady-state and steady-state kinetics and turnover rate of the mouse gamma-aminobutyric acid transporter (mGAT3). *J Membr Biol* **190**, 57–73.

Saparov SM, Kozono D, Rothe U, Agre P & Pohl P (2001). Water and ion permeation of aquaporin-1 in planar lipid bilayers. Major differences in structural determinants and stoichiometry. *J Biol Chem* **276**, 31515–31520.

Sasaki S, Ishibashi K, Nagai T & Marumo F (1992). Regulation mechanisms of intracellular pH of *Xenopus laevis* oocyte. *Biochim Biophys Acta* **1137**, 45–51.

Schmolke M, Bornemann A & Guder WG (1990). Polyol determination along the rat nephron. *Biol Chem Hoppe Seyler* **371**, 909–916.

Smith-Maxwell C, Bennett E, Randles J & Kimmich GA (1990). Whole cell recording of sugar-induced currents in LLC-PK1 cells. *Am J Physiol Cell Physiol* **258**, C234–C242.

Spector R & Lorenzo AV (1975). Myo-inositol transport in the central nervous system. *Am J Physiol* **228**, 1510–1518.

Trachtman H (1992). Cell volume regulation: a review of cerebral adaptive mechanisms and implications for clinical treatment of osmolal disturbances. II. *Pediatr Nephrol* **6**, 104–112.

Tsunoda SP, Wiesner B, Lorenz D, Rosenthal W & Pohl P (2004). Aquaporin-1, nothing but a water channel. *J Biol Chem* **279**, 11364–11367.

Turner RJ & Moran A (1982). Stoichiometric studies of the renal outer cortical brush border membrane D-glucose transporter. *J Membr Biol* **67**, 73–80.

Uldry M, Ibberson M, Horisberger JD, Chatton JY, Riederer BM & Thorens B (2001). Identification of a mammalian H^+-myo-inositol symporter expressed predominantly in the brain. *EMBO J* **20**, 4467–4477.

Uldry M, Steiner P, Zurich MG, Beguin P, Hirling H, Dolci W *et al*. (2004). Regulated exocytosis of an H^+/myo-inositol symporter at synapses and growth cones. *EMBO J* **23**, 531–540.

Weiss JN (1997). The Hill equation revisited: uses and misuses. *FASEB J* **11**, 835–841.

Wiese TJ, Dunlap JA, Conner CE, Grzybowski JA, Lowe WL Jr & Yorek MA (1996). Osmotic regulation of Na-myo-inositol cotransporter mRNA level and activity in endothelial and neural cells. *Am J Physiol Cell Physiol* **270**, C990–C997.

Yamauchi A, Sugiura T, Ito T, Miyai A, Horio M, Imai E *et al*. (1996). Na^+/myo-inositol transport is regulated by basolateral tonicity in Madin–Darby canine kidney cells. *J Clin Invest* **97**, 263–267.

Yool AJ, Stamer WD & Regan JW (1996). Forskolin stimulation of water and cation permeability in aquaporin 1 water channels. *Science* **273**, 1216–1218.

Zampighi GA, Kreman M, Boorer KJ, Loo DD, Bezanilla F, Chandy G *et al*. (1995). A method for determining the unitary functional capacity of cloned channels and transporters expressed in *Xenopus laevis* oocytes. *J Membr Biol* **148**, 65–78.

Zhang X & Majerus PW (1998). Phosphatidylinositol signalling reactions. *Semin Cell Dev Biol* **9**, 153–160.

Zhang XM, Wang XT, Yue H, Leung SW, Thibodeau PH, Thomas PJ *et al*. (2003). Organic solutes rescue the functional defect in delta F508 cystic fibrosis transmembrane conductance regulator. *J Biol Chem* **278**, 51232–51242.

Acknowledgements